

# On the Construction of POD Models from Partial Observations

(Invited Paper)

Patricia Astrid and Siep Weiland

**Abstract**—This paper discusses the use of partial state observations in the construction of reduced order models based on proper orthogonal decompositions (POD). A main motivation for this work lies in the observation that reductions of the state dimension of large scale nonlinear and time-varying models hardly enhances the computational speed of these models. It is shown that information from output variables or sampled state information can be used in an efficient manner to accelerate computation speed in reduced order models while allowing state recovery properties in an exact or approximate sense.

## I. INTRODUCTION

The method of Proper Orthogonal Decomposition (POD) has become a popular reduction method. The method aims to characterize dominant dynamical features of a system by extracting persistent structural patterns in observed data. First experimental research to find and characterize such patterns in turbulent flows have been reported in [5]. POD applications have been reported in computational fluid dynamics [8], [4], aerodynamics, oceanography, etc. The POD method identifies modes (or basis functions) by optimally capturing the average energy content of experimental data in a 2-norm sense. Unlike other methods that use spectral decompositions, the POD method is data driven and defines an *empirical* spectral decomposition of signals.

This paper discusses the construction of reduced order models by projecting the state on a suitably defined subspace inferred from partial observations of the state. In addition, we address the problem of state recovery from an arbitrary sampled spatial domain. It is shown that alias effects can be minimized by an appropriate choice of samples from which the reduced order model can be build. Two criteria are proposed to identify such samples. This method leads to models in which the computational speed has been accelerated by a factor of about 7.

The paper is organized as follows. A brief introduction to POD will be presented first and the introduction of the method used to construct a reduced model based on partial observation will follow. Subsequently, propositions of deriving POD basis from other criteria will also be discussed. Finally, applications of some of the proposed methods on an industrially relevant process will be shown in the last section.

P. Astrid is with the Control Systems Group, Department of Electrical Engineering, Eindhoven University of Technology, 5600 MB Eindhoven, The Netherlands p.astrid@tue.nl

S. Weiland is with the Control Systems Group, Department of Electrical Engineering, Eindhoven University of Technology, 5600 MB Eindhoven, The Netherlands s.weiland@tue.nl

## II. PROPER ORTHOGONAL DECOMPOSITION

The method of proper orthogonal decompositions (POD) amounts to choosing an optimal basis of the space in which the physical variables reside. Let  $\mathbb{T} \subseteq \mathbb{R}$  be a time set and suppose that for any time  $t \in \mathbb{T}$ , an observed variable  $\mathbf{w}(t)$  belongs to a separable Hilbert space  $\mathcal{X}$ . Further, let  $\mathcal{T}$  denote a Hilbert space of time dependent functions mapping  $\mathbb{T}$  to  $\mathbb{R}$ . Throughout, inner products and norms are denoted by  $(\cdot, \cdot)$  and  $\|\cdot\|$ , and subscripted by the Hilbert space whenever the context requires this.

For any orthonormal basis  $\{\varphi_i\}_{i \in \mathbb{I}}$  of  $\mathcal{X}$  with  $\mathbb{I}$  some countable index set, the observation  $\mathbf{w}(t)$  (the  $t$ th *snapshot*) admits a spectral expansion

$$\mathbf{w}(t) = \sum_{i \in \mathbb{I}} a_i(t) \varphi_i \quad (1)$$

where  $a_i(t) := (\varphi_i, \mathbf{w}(t))$  is the  $i$ th *modal coefficient* of the expansion (1). Here, convergence of the series (1) is understood in the strong sense when  $\lim_{n \rightarrow \infty} \|\mathbf{w}_n(t) - \mathbf{w}(t)\| = 0$ ,  $t \in \mathbb{T}$ , where

$$\mathbf{w}_n(t) = \sum_{i=1}^n a_i(t) \varphi_i \quad (2)$$

is the  $n$ th partial sum.

Given an ensemble of observations  $\{\mathbf{w}(t)\}_{t \in \mathbb{T}}$ , a *POD basis* is an orthonormal basis  $\{\varphi_k\}_{k \in \mathbb{I}}$  of  $\mathcal{X}$  with the property that the truncation error

$$\|\mathbf{w} - \mathbf{w}_n\| := \left\| \left( \sum_{k > n} a_k^2(t) \right)^{1/2} \right\|_{\mathcal{T}}$$

is minimal for all truncation levels  $n$ . Equivalently, the modal coefficients  $a_i(t)$  of  $\mathbf{w}(t)$  are ordered according to  $\|a_k\|_{\mathcal{T}} \geq \|a_\ell\|_{\mathcal{T}}$  whenever  $k \leq \ell$ .

A POD basis is obtained by constructing the data-correlation map  $C : \mathcal{X} \rightarrow \mathcal{X}$  defined by

$$(\psi_1, C\psi_2) = ((\psi_1, w)_{\mathcal{X}}, (\psi_2, w)_{\mathcal{X}})_{\mathcal{T}}. \quad (3)$$

Then  $C$  is self-adjoint and non-negative definite and a POD basis consists of the (normalized) eigenfunctions of  $C$  and the error

$$\|\mathbf{w} - \mathbf{w}_n\|^2 = \sum_{i > n} \lambda_i$$

where  $\lambda_i$  is the  $i$ th largest eigenvalue of  $C$ . Clearly, if  $\mathcal{X}$  is finite dimensional then a POD basis is readily inferred from a singular value decomposition of the matrix  $C$ .

POD bases have found main applications in the reduction of models described by partial differential equations. These

models consist of spatial temporal signals  $w : \mathbb{X} \times \mathbb{T} \rightarrow \mathbb{R}$  described by partial differential equations of the form

$$R(\partial_x, \partial_t)(w) = 0. \quad (4)$$

Here,  $\mathbb{X} \subset \mathbb{R}^d$  is a (compact) configuration space of spatial coordinates,  $\mathbb{T} \subseteq \mathbb{R}$  is the time set,  $\partial_x = \partial_{x_1}, \dots, \partial_{x_d}$  where  $\partial_{x_i}$  denotes the partial derivative with respect to the  $i$ th spatial coordinate,  $\partial_t$  is the partial derivative with respect to time and  $R$  is an operator.

A variational formulation of the solution concept of (4) leads to expressions for the modal coefficients  $a_i$  in the expansions (1) and (2). Specifically, the *Galerkin projection* amounts to defining the reduced order model of complexity  $n$  as to consist of all functions  $w_n : \mathbb{X} \times \mathbb{T} \rightarrow \mathbb{R}$  for which

- $\mathbf{w}_n(t) := w_n(\cdot, t)$  belongs to  $\mathcal{X}$  for all  $t \in \mathbb{T}$
- $\mathbf{w}_n(t)$  admits an expansion (2) with POD basis  $\{\varphi_i\}_{i=1}^n$ .
- the variational expression

$$(R(\partial_t, \partial_x)w_n, \varphi) = 0 \quad (5)$$

for all  $\varphi \in \mathcal{X}_n = \text{span}(\varphi_1, \dots, \varphi_n)$ .

Substitution of the expansion (2) in (5) yields a set of  $n$  differential equations in the modal coefficients  $a_i$ . These may be linear or nonlinear, implicit or explicit, time-varying or time-invariant depending on particular properties of  $R$ .

### III. MISSING POINT ESTIMATION

For nonlinear and time-varying systems, the Galerkin projection (5) is a formidable task, even for low values of  $n$  as it involves evaluations of the residual of  $R$  and evaluations of the inner product in  $\mathcal{X}$ . The objective of this section is to formalize a theoretical basis for the calculation of the evolution of modal coefficients  $a_i$  in (2) based on *partial observations*.

The approach is also referred to as the Missing Point Estimation (MPE) and inspired by the *Gappy POD* approach proposed by Everson and Sirovich [7]. The method has been applied to recover missing data from a static image [7], fluid flow reconstruction and sensing [6], [12]. In this paper, the approach is generalized and developed for dynamical systems.

We will consider two cases. The first one amounts to exact reconstruction of modal coefficients from sampled data or sampled measurements. The second case amounts to the approximate recovery of signals from sampled values.

#### A. Exact reconstruction

Suppose that  $\mathbb{X}_0$  is a finite subset of  $N$  distinct points  $\mathbb{X}_0 = \{x_1, \dots, x_N\}$  in the configuration domain  $\mathbb{X}$ . Suppose that the points  $\mathbb{X}_0$  represent the measured states or locations or, alternatively, a sampling of the spatial domain  $\mathbb{X}$  in  $N$  samples. A *measurement* or *partial observation* is a function  $\tilde{w} : \mathbb{X}_0 \times \mathbb{T} \rightarrow \mathbb{R}$  defined on samples  $\mathbb{X}_0$  and time  $\mathbb{T}$  and satisfies the restriction  $\tilde{w} = w|_{\mathbb{X}_0 \times \mathbb{T}}$  for some (unobserved) signal  $w : \mathbb{X} \times \mathbb{T} \rightarrow \mathbb{R}$ .

Let  $\{\varphi_k\}_{k \in \mathbb{I}}$  be a basis for the Hilbert space  $\mathcal{X}$  and let  $\tilde{\varphi}_k = \varphi_k|_{\mathbb{X}_0}$  be the restriction of the basis elements to the samples  $\mathbb{X}_0$ . Define, for  $n > 0$ , the expansion

$$\tilde{w}_n(x, t) := \sum_{k=1}^n \tilde{a}_k(t) \tilde{\varphi}_k(x), \quad x \in \mathbb{X}_0, t \in \mathbb{T} \quad (6)$$

for a suitable set of modal coefficients  $\{\tilde{a}_k\}_{k=1}^n$  with  $\tilde{a}_k : \mathbb{T} \rightarrow \mathbb{R}$ .

Given such a set of modal coefficients  $\{\tilde{a}_k\}_{k=1}^n$ , its *interpolation* is the signal

$$\hat{w}_n(x, t) := \sum_{k=1}^n \tilde{a}_k(t) \varphi_k(x), \quad x \in \mathbb{X}, t \in \mathbb{T} \quad (7)$$

defined on all of  $\mathbb{X} \times \mathbb{T}$ . Note that  $\hat{w}_n$  coincides with  $\tilde{w}_n$  on the sample points and on all time instants  $t \in \mathbb{T}$ .

Also, introduce the matrix  $\tilde{\Phi} \in \mathbb{R}^{N \times n}$  of samples of the first  $n$  basis elements according to

$$\tilde{\Phi} := \begin{pmatrix} \varphi_1(x_1) & \dots & \varphi_n(x_1) \\ \vdots & & \vdots \\ \varphi_1(x_N) & \dots & \varphi_n(x_N) \end{pmatrix}. \quad (8)$$

Then (6) can be written in matrix form as

$$\tilde{\mathbf{w}}_n(t) := \tilde{\Phi} \tilde{\mathbf{a}}(t)$$

where  $\tilde{\mathbf{a}}(t) = \text{col}(\tilde{a}_1(t), \dots, \tilde{a}_n(t))$  is the vector of coefficients.

Since  $\{\varphi_k\}_{k \in \mathbb{I}}$  is a basis of  $\mathcal{X}$ , it is immediate that for  $n$  sufficiently large, the matrix  $\tilde{\Phi}$  will be *surjective*. Consequently, for  $n$  sufficiently large, the partial observation  $\tilde{w}$  coincides with  $\tilde{w}_n$  by taking  $\tilde{\mathbf{a}}(t) = \tilde{\Phi}^{-R} \tilde{\mathbf{w}}(t)$  with  $\tilde{\Phi}^{-R} = \tilde{\Phi}^\top (\tilde{\Phi} \tilde{\Phi}^\top)^{-1}$  the right inverse of  $\tilde{\Phi}$  and  $\tilde{\mathbf{w}}(t) = \text{col}(\tilde{w}(x_1, t), \dots, \tilde{w}(x_N, t))$  the vector of observations.

Similarly, if  $\tilde{\Phi}$  is *injective*, the coefficient vector

$$\tilde{\mathbf{a}}(t) = \tilde{\Phi}^{-L} \tilde{\mathbf{w}}(t) \quad (9)$$

where  $\tilde{\Phi}^{-L} = (\tilde{\Phi}^\top \tilde{\Phi})^{-1} \tilde{\Phi}^\top$  is the left inverse of  $\tilde{\Phi}$  is the unique vector that achieves  $\tilde{w}_n = \tilde{w}$  provided that  $\tilde{\mathbf{w}}(t)$  lies in the image of  $\tilde{\Phi}$  for all  $t \in \mathbb{T}$ .

Now introduce on  $\mathcal{X}$  the bilinear form

$$(\varphi, \psi)_N := \sum_{i,j=1}^N \varphi(x_i) q_{i,j} \psi(x_j), \quad \varphi, \psi \in \mathcal{X} \quad (10)$$

where  $q_{i,j}$  is the  $(i, j)$ -th entry of the real symmetric matrix  $Q \in \mathbb{R}^{N \times N}$ :

$$Q := \tilde{\Phi} \left( \tilde{\Phi}^\top \tilde{\Phi} \right)^{-2} \tilde{\Phi}^\top.$$

We then have the following result on exact signal reconstruction.

*Theorem 1:* Given a set  $\mathbb{X}_0 = \{x_1, \dots, x_N\}$  of  $N$  distinct samples, and an orthonormal basis  $\{\varphi_k\}_{k \in \mathbb{I}}$  of  $\mathcal{X}$ . Suppose  $\tilde{\Phi}$  has rank  $n$ . If  $w \in \mathcal{X}_n = \text{span}(\varphi_1, \dots, \varphi_n)$  then  $w$  can be reconstructed exactly from its partial observations  $\tilde{w} = w|_{\mathbb{X}_0 \times \mathbb{T}}$  in that

$$\hat{w}_n(x, t) = w(x, t) \quad \text{for all } x \in \mathbb{X}, t \in \mathbb{T},$$

by taking expansion coefficients

$$\tilde{a}_k = (w, \varphi_k)_N, \quad k = 1, \dots, n$$

in the interpolant (7).

*Proof:* The proof is based on the observation that

$$(\varphi, \psi)_N = (\varphi, \psi)_{\mathcal{X}} \quad \text{for all } \varphi, \psi \in \mathcal{X}_n$$

whenever  $\tilde{\Phi}$  is injective. Indeed, with expansions  $\varphi = \sum_{k=1}^n a_k \varphi_k$  and  $\psi = \sum_{k=1}^n b_k \varphi_k$ , we infer that

$$\begin{aligned} (\varphi, \psi) &= \sum_{k=1}^n a_k b_k = \mathbf{a}^\top \mathbf{b} = \tilde{\psi}^\top \tilde{\Phi}^{-L} \tilde{\Phi}^{-L} \tilde{\varphi} \\ &= (\varphi, \psi)_N \end{aligned}$$

where boldface is used to denote vectors. In particular, this implies that the bilinear form (10) defines an inner product on  $\mathcal{X}_n$  whenever  $\tilde{\Phi}$  is injective. If  $w \in \mathcal{X}_n$  then  $w$  admits an expansion of the form (2) whose coefficients satisfy

$$a_k = (w, \varphi_k) = (w, \varphi_k)_N = \tilde{a}_k, \quad k = 1, \dots, n$$

i.e., the modal coefficients of  $w$  coincide with the modal coefficients of  $\hat{w}_n$  in (7). But then  $w = \hat{w}_n$ , as desired. ■

It is important to observe that, by (10), the coefficients  $\tilde{a}_k(t) = (w(\cdot, t), \varphi_k)_N$  in Theorem 1 can be determined from the samples  $\tilde{w}$  and  $\tilde{\varphi}_k$  only. Hence, no information of  $w$  other than its partial observations is necessary to recover  $w$  from its samples, provided  $w \in \mathcal{X}_n$  and  $\tilde{\Phi}$  has rank  $n$ .

### B. Approximate reconstruction

In the general case,  $w \notin \mathcal{X}_n$  and exact signal reconstruction on the basis of partial information  $\tilde{w}$  on the samples will not be possible. As in Theorem 1, let

$$\tilde{a}_k(t) = (w(\cdot, t), \varphi_k)_N, \quad t \in \mathbb{T}, k = 1, \dots, n$$

denote the modal coefficients determined from the partial observation of  $w$  and let  $\hat{w}_n$  denote its corresponding interpolant (7). Let  $\{a_k\}_{k \in \mathbb{I}}$  be the coefficients in the expansion (1) of  $w$ . Then a straightforward calculation shows that

$$\tilde{a}_k = a_k + \sum_{\ell > n} a_\ell (\varphi_\ell, \varphi_k)_N, \quad k = 1, \dots, n$$

i.e.,  $\tilde{a}_k$  not only depends on  $a_k$  but also on higher order coefficients  $a_\ell$  of  $w$  with  $\ell > n$ . This is generally referred to as *aliasing*. Furthermore, the error between  $w$  and the interpolant  $\hat{w}$  is given by

$$\begin{aligned} \|w - \hat{w}_n\|_{\mathcal{X}}^2 &= \|w - w_n\|^2 + \|w - \hat{w}_n\|^2 \\ &= \sum_{k > n} a_k^2 + \sum_{k=1}^n \left( \sum_{\ell > n} a_\ell (\varphi_\ell, \varphi_k)_N \right)^2 \end{aligned}$$

and is therefore decomposed in a projection error  $\|w - w_n\|$  and an alias error  $\|w_n - \hat{w}_n\|$ . The alias error is therefore represented by the *alias operator*  $A_n$ , mapping square summable sequences (elements in  $\ell_2(\mathbb{I}, \mathbb{R})$ ) to  $\mathbb{R}^n$  according to

$$A_n a := \text{col} \left( \sum_{\ell > n} a_\ell (\varphi_\ell, \varphi_k)_N, k = 1, \dots, n \right)$$

Its induced norm

$$\|A_n\| := \sup_{0 \neq a \in \ell_2(\mathbb{I}, \mathbb{R})} \frac{\|A_n a\|}{\|a\|}$$

is a measure of the *alias sensitivity* and characterized as follows.

*Theorem 2:* The alias sensitivity  $\|A_n\| = \lambda_{\max}^{1/2}(A_n A_n^*)$  where  $A_n A_n^*$  is the  $n \times n$  matrix whose  $(k, \ell)$ th entry is given by

$$(A_n A_n^*)_{k, \ell} = \sum_{p > n} (\varphi_p, \varphi_k)_N \cdot (\varphi_p, \varphi_\ell)_N$$

If  $\mathcal{X}$  is finite dimensional with standard Euclidean inner product, then

$$A_n A_n^* = (\tilde{\Phi}^\top \tilde{\Phi})^{-1} - I.$$

*Proof:* The adjoint  $A_n^* : \mathbb{R}^n \rightarrow \ell_2(\mathbb{I}, \mathbb{R})$  is given by

$$(A_n^* b)(\ell) := \begin{cases} 0 & \text{if } 1 \leq \ell \leq n \\ \sum_{k=1}^n b_k (\varphi_\ell, \varphi_k)_N & \text{if } \ell \in \mathbb{I}, \ell > n \end{cases}$$

The first part of the theorem then follows by rewriting  $(e_k, A_n A_n^* e_\ell) = (A_n^* e_k, A_n^* e_\ell)$ . The second part requires a lengthy algebraic derivation that we omit here. ■

## IV. SELECTION OF SAMPLE POINTS

By Theorem 2, the minimization of the alias sensitivity  $\|A_n\|$  is equivalent to the minimization of  $\|A_n A_n^*\|$  or, if  $\mathcal{X}$  is finite dimensional, to the minimization of

$$\|(\tilde{\Phi}^\top \tilde{\Phi})^{-1} - I\|$$

over all possible choices of  $N$  sample points  $\mathbb{X}_0$  from  $\mathbb{X}$ . This is a combinatorial optimization problem and its solution is of evident practical interest to determine suitable sensor locations in a spatial configuration. In this section we propose two algorithms for the selection of  $N$  sample points that are sub-optimal solutions to this problem, but avoid a combinatorial search. In this section it is assumed that  $\mathcal{X}$  is finite dimensional, or, equivalently, the configuration space  $\mathbb{X}$  is assumed to be gridded in a finite (and possibly large) number of grids. We suppose that  $K = \dim(\mathcal{X})$  and recall that  $\tilde{\Phi}$  depends on  $\mathbb{X}_0$  through (8).

### A. Point selection criterion 1

The norm that we will use to characterize  $\mathbb{X}_0$  in this point selection criterion is defined for a square matrix  $X \in \mathbb{R}^{n \times n}$  as:

$$\|X\| = \sum_{i, j=1}^n X_{ij}^2 \quad (11)$$

where  $X_{ij}$  represents the  $(i, j)$ th entry of  $X$ . Furthermore, if  $X$  is symmetric and positive definite the *condition number* of  $X$  is defined as  $c(X) = \frac{\lambda_{\max}(X)}{\lambda_{\min}(X)}$ . Obviously, the condition number  $c(X) \geq 1$ .

The quality of a particular grid or sample set  $\mathbb{X}_0$  will be expressed in terms of the condition number  $c(\mathbb{X}_0) := c(\tilde{\Phi}^\top \tilde{\Phi})$  and a measure  $e(\mathbb{X}_0)$  defined as

$$e(\mathbb{X}_0) = \|\tilde{\Phi}^\top \tilde{\Phi} - I\| \quad (12)$$

where  $\|\cdot\|$  is defined in (11). By Theorem 2, the closer  $c(\mathbb{X}_0)$  to 1 and the smaller  $e(\mathbb{X}_0)$ , the smaller the alias sensitivity will be.

Obviously,  $e(\mathbb{X}_0) = 0$  if  $\mathbb{X}_0 = \mathbb{X}$  and a grid  $\mathbb{X}'_0$  is considered better than  $\mathbb{X}''_0$  whenever they have the same cardinality and

$$e(\mathbb{X}'_0) \leq e(\mathbb{X}''_0).$$

The case where  $\mathbb{X}_0$  consists of one point only, i.e.,  $\mathbb{X}_0 = \{x_k\}$  is of special interest as it enables an ordering of all points in  $\mathbb{X}$ . We calculate  $e(x_k)$  for every point  $x_k$  in  $\mathbb{X}$ , and re-order the points in  $\mathbb{X}$  such that

$$e(x_{k_1}) \leq e(x_{k_2}) \leq \dots \leq e(x_{k_K}) \quad (13)$$

with  $k_1, k_2, \dots, k_K$  the re-ordered indices. With  $N < K$  and a tolerance  $c_{\text{tol}} \geq 1$ , the set  $\mathbb{X}_0$  consists of the first  $N$  points in the sequence  $\{x_{k_1}, \dots, x_{k_K}\}$  (incrementally determined) such that the condition number  $c(\mathbb{X}_0) \leq c_{\text{tol}}$ .

### B. Point selection criterion 2

As a second selection criterion for  $\mathbb{X}_0$ , consider the ensemble of projected signals  $\mathbf{w}_n(t)$ ,  $t \in \mathbb{T}$ , as defined in (2) and let

$$\mathbf{W}_n := (\mathbf{w}_n(t_1) \quad \dots \quad \mathbf{w}_n(t_M))$$

where  $M$  is the number of time samples in  $\mathbb{T}$ . Let  $\Pi_{\mathbb{X}_0}$  denote the canonical projection from  $\mathbb{X}$  to  $\mathbb{X}_0$  and define, for all time instants  $t \in \mathbb{T}$ , the projections  $\bar{\mathbf{w}}_n(t) = \Pi_{\mathbb{X}_0} \mathbf{w}_n(t)$ . Now set

$$\bar{\mathbf{W}}_n := (\bar{\mathbf{w}}_n(t_1) \quad \dots \quad \bar{\mathbf{w}}_n(t_M)).$$

We will consider the temporal correlation matrices  $\mathbf{W}_n^\top \mathbf{W}_n$  and  $\bar{\mathbf{W}}_n^\top \bar{\mathbf{W}}_n$  and define the criterion  $e(\mathbb{X}_0)$  by

$$e(\mathbb{X}_0) = \|\mathbf{W}_n^\top \mathbf{W}_n - \bar{\mathbf{W}}_n^\top \bar{\mathbf{W}}_n\| \quad (14)$$

The norm  $\|\cdot\|$  is again defined by (11). When compared to the criterion in subsection IV-A, this criterion explicitly takes the measured data into account. As before, the quantity  $e(\mathbb{X}_0)$  is calculated for singletons  $\mathbb{X}_0 = \{x_k\}$ , i.e., we determine  $e(x_k)$  for every point  $x_k$  in  $\mathbb{X}$  and then re-order the points as in (13).

Again, given  $N < K$  and a tolerance  $c_{\text{tol}} \geq 1$ , the set  $\mathbb{X}_0$  consists of the first  $N$  points in the sequence  $\{x_{k_1}, \dots, x_{k_K}\}$  (incrementally determined) such that the condition number  $c(\mathbb{X}_0) \leq c_{\text{tol}}$ .

## V. INCORPORATION OF MEASUREMENTS IN POD BASIS

In practice, measurements are often not conducted in the regions that are excited by the input signals. With such non-collocated measurements, there is no a priori guarantee that these points are relevant for the purpose of model approximation, as they may have poor state estimation properties.

rement points are considered more important than the state variables, the approximations by POD basis may fail when the points are not contributing significantly to the overall spatial dynamics.

We propose an approach to extract the contribution of *measurements* in the construction of POD basis functions.

Note that we do not consider the balanced-POD method as described in [10], since it requires collections of impulse response data, which may not be allowed in specific physical systems.

Here, we decompose  $\mathbf{w}(t)$  as:

$$\mathbf{w}(t) = \mathbf{w}_o(t) + \mathbf{w}_u(t)$$

where  $\mathbf{w}_o \in \mathbb{R}^K$  is the vector of *observed* or measured state variables. The vector  $\mathbf{w}_u := \mathbf{w}(t) - \mathbf{w}_o(t)$  refers to the vector of *unmeasured state variables*. It is assumed that we have somehow access to the unmeasured variables, e.g., through a mathematical model.

The approach we introduce here is inspired by the derivation of POD basis with *Maximum Noise Fraction* (MNF) [9]. In the MNF method, the eigenvectors of the noise signals are filtered to obtain a set of basis vectors with a minimum contribution of noise and a maximum contribution of the signals. Analogously, we can view this as a means to filter the POD basis with *maximum output fraction*.

As before, each element of the POD basis can be written as a linear combination of the snapshot  $\{\mathbf{w}(t)\}_{t \in \mathbb{T}}$  as

$$\varphi_k = \psi_{i,1} \mathbf{w}(t_1) + \dots + \psi_{k,M} \mathbf{w}(t_M) = \mathbf{W}_{\text{snap}} \boldsymbol{\psi}_k. \quad (15)$$

The POD basis is said to have *Maximum Output Fraction* if the ratio

$$D(\boldsymbol{\psi}) = \frac{\boldsymbol{\psi}^\top \mathbf{W}_o^\top \mathbf{W}_o \boldsymbol{\psi}}{\boldsymbol{\psi}^\top \mathbf{W}_{\text{snap}}^\top \mathbf{W}_{\text{snap}} \boldsymbol{\psi}} \quad (16)$$

is maximum. Here,

$$\mathbf{W}_o = (\mathbf{w}_o(t_1) \quad \dots \quad \mathbf{w}_o(t_M))$$

and

$$\mathbf{W}_{\text{snap}} = (\mathbf{w}(t_1) \quad \dots \quad \mathbf{w}(t_M)).$$

The maximum of (16) is found by differentiating (16) to  $\boldsymbol{\psi}$  and set the result to zero. It turns out that this is equivalent to solving a *symmetric definite generalized eigenproblem*. The set of the basis functions which maximizes (16) and minimizes the mean-averaged projection error are found by solving the generalized eigenproblem (17):

$$\mathbf{W}_o^\top \mathbf{W}_o \boldsymbol{\psi} = \mu^2 \mathbf{W}_{\text{snap}}^\top \mathbf{W}_{\text{snap}} \boldsymbol{\psi} \quad (17)$$

The eigenvalues  $\{\mu_j^2\}_{j=1}^L$ ,  $L \ll K$  describe the contribution of each basis function  $\boldsymbol{\psi}_j$ . The basis function  $\boldsymbol{\psi}_1$  is the one with the maximum contribution of the measured output dynamics and the last basis function  $\boldsymbol{\psi}_L$  is the one with the minimum contribution of the measured output dynamics.

The basis functions  $\varphi_k$  are now selected corresponding to the  $n$  largest generalized singular values  $\mu_j$  according to (15).

## VI. APPLICATIONS

### A. The original model

The original model here is a model of a glass melt feeder. Glass melt feeder is a section of a glass melting furnace where the temperature distribution has to be controlled very

tightly [3]. The governing equation for the temperature distribution  $w$  is given by:

$$\frac{\partial(\rho c_p w)}{\partial t} = -\text{div}(\rho c_p w \mathbf{u}) + \text{div}(\kappa \text{grad} w) + q \quad (18)$$

where  $\rho$  is the density, which is temperature dependent for glass,  $c_p$  is the heat-capacity,  $\kappa$  is the heat conductivity which is also temperature dependent for glass, and  $q$  is the external energy sources applied to the feeder. In this paper, we only consider the *reduced order modeling of the temperature distribution*. The mass and momentum balances are calculated by the original model.

Discretization of (18) using the Finite Volume Method [11], [1] results in the following linear time varying (LTV) systems:

$$\mathbf{A}(t_j) \mathbf{w}(t_j) = \mathbf{A}_0(t_j) \mathbf{w}(t_j) + \mathbf{B}(t_j) \mathbf{u}(k) \quad (19)$$

where  $\mathbf{w}(t_j) \in \mathbb{R}^K$  is the unknown variable and the spatial domain is discretized into  $K$  grid cells. The matrices  $\mathbf{A}(t_j) \in \mathbb{R}^{K \times K}$ ,  $\mathbf{A}_0(t_j) \in \mathbb{R}^{K \times K}$ ,  $\mathbf{B}(t_j) \in \mathbb{R}^{K \times n_u}$  are time varying since they are functions of the temperature-dependent physical parameters such as density and heat conductivity. The input signals which represent here the zones of the crown temperature is stored in  $\mathbf{u}(kt_j) \in \mathbb{R}^{n_u}$ . The model we consider here are discretized into 3800 grid cells,  $K = 3800$ . The crown is divided into four zones, so  $n_u = 4$ . The boundary conditions along the feeder width are symmetric, so we only consider  $K = 1900$  in the calculation of the original model.

During the production process, the temperature distribution of the crown is varied from its nominal distribution (which has a temperature range of 1450-1500 K) in every zone. The variations are depicted in Fig. 1. We simulate

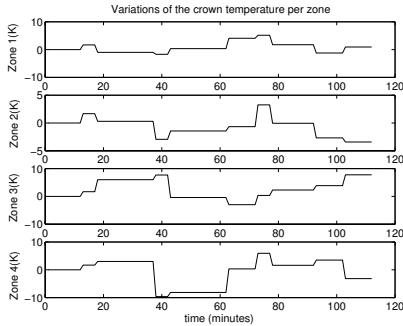


Fig. 1. The variations of the crown temperature

here the process of glass color change in the glass feeder from green to transparent under the subsection of the crown temperature variations as shown in Fig. 1. As a result of this color change process, the temperature distribution will significantly change as the heat conductivity will change about 8 times higher. The POD basis is derived from the temperature data collected for 112 minutes. Eighteen POD basis functions corresponding to 18 largest eigenvalues are chosen to construct the POD reduced order model by projecting  $\Phi = \{\varphi_i\}_{i=1}^{18}$  onto (19). This results in an 18-order reduced order model.

## B. Acceleration by MPE

Computationally, the reduced order model is only about 2.2 times faster than the original model. To enhance the computational speed, the MPE technique as described in Section III is applied. Representative grid points are chosen based on the two criteria proposed in Section III.

First, since we have to obtain information from the excitation signals, we select the grid points located adjacent to the locations where excitation signals such as the crown temperature are defined. There are 265 grid points which are adjacent to the excitation signal locations. The remaining points are chosen based on the ordering introduced in Section IV-A and Section IV-B. The number of points which characterize  $\mathbb{X}_0$  are taken such that the condition number of  $\tilde{\Phi}^\top \tilde{\Phi}$  is low to ensure good estimation of the POD coefficients. After employing the MPE criterion 1, a total of 665 representative grid points out of 1900 points are chosen while 1465 grid points are chosen after applying the MPE criterion 2.

The reduced models are constructed by projecting the equations of the points in  $\mathbb{X}_0$  onto  $\{\tilde{\Phi}_k\}_{k=1}^{18}$  defined on  $\mathbb{X}_0$ :

$$\tilde{\Phi}^\top \tilde{\mathbf{A}}(t_j) \tilde{\mathbf{a}}(t_j) = \tilde{\Phi}^\top \tilde{\mathbf{A}}_0(t_j) \tilde{\Phi}(t_j) + \tilde{\Phi}^\top \mathbf{B}(t_j) \mathbf{u}(t_j) \quad (20)$$

Derivation details can be found in [1]. Note that we still obtain a reduced order model of order 18 but through a cheaper procedure since we construct it from a part of the original equations.

The reduced order models are validated by imposing a random excitation signals for every temperature zone as plotted in Fig. 2. Fig. 3 shows the response at a measurement

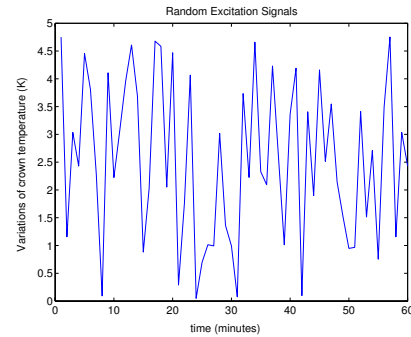


Fig. 2. The random excitation signal used to validate the reduced order model

location under the random excitations and the reduced order models constructed by MPE criterion 1 and MPE criterion 2. Though the reduced order model by MPE criterion 1 is only based on 665 points, it performs better than the reduced order model built by MPE criterion 2 built from 1465 points. The condition number of  $\tilde{\Phi}^\top \tilde{\Phi}$  is lower for MPE-criterion 1 and this results in a better estimate of the POD coefficients. Thus for this case, MPE criterion 1 is a more effective selection criterion. The model constructed by MPE criterion 1 is 5.27 times faster than the original model which correspond to 6 times faster than real time while the one with MPE criterion 2 is only 2.89 faster than the original model. It is possible to optimize both point selection procedure that we can construct

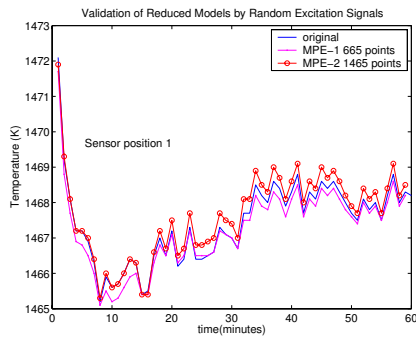


Fig. 3. Responses of reduced and original models under random excitation

$\mathbb{X}_0$  based on less number of points by implementing the greedy algorithm as explained in [2] and [12].

Table I summarizes the performance of both MPE models.

TABLE I  
COMPARISON BETWEEN MPE MODELS FOR RANDOM EXCITATIONS.

Model Type	Maximum Absolute Average Error	Condition number	Gain
MPE-1 (665 points)	0.486 K	7	527%
MPE-2 (1465 points)	0.897 K	24.2	289%

### C. Construction of POD basis with Maximum Output Fraction

POD basis can also be derived by maximizing the contribution from the measured variables as presented in section V. In this example, there are six measurement locations on the surface of the glass melt. The generalized eigenvalue problem (17) is solved and the eigenvalue spectrum is shown in Fig. 4. There is a large gap in the eigenvalue spectrum after the 6-th eigenvalue which indicates that the dynamics of these six measured state variables do not contribute significantly to the overall dynamics.

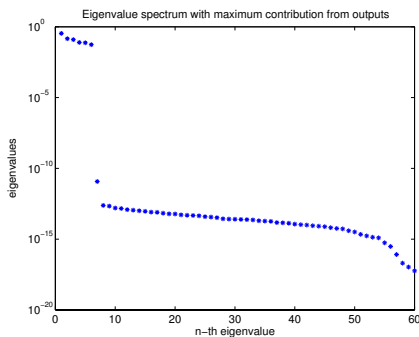


Fig. 4. Eigenvalue spectrum of POD basis with maximum output fraction

Fig. 5 shows that the dynamics a measured state variable can be reconstructed very well by the 6 POD basis functions derived from the Maximum Output Fraction approach while the first 6 conventional POD basis functions give worse approximations.

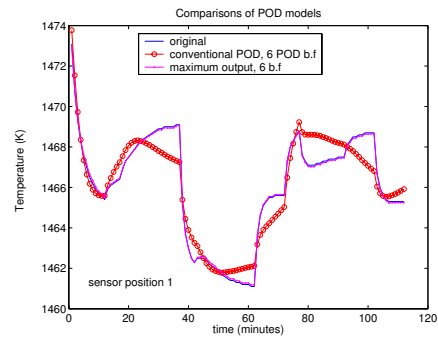


Fig. 5. Estimation of measured variables by conventional and Maximum Output Fraction POD basis

## VII. CONCLUSION

We have presented several approaches to modify the POD reduced order modeling by using partial observations of the state variables. The partial observations can be used to construct fast POD reduced order models for nonlinear and time-varying models as the reduced order models are obtained by projecting the equations governing the observed state variables only onto the POD basis functions. Further, we can also derive POD basis functions by maximizing the contributions from the measured state variables or the variables which are considered more important than the others. It results in better and efficient approximations of the variables we are particularly interested in.

## REFERENCES

- [1] P. Astrid. *Reduction of process simulation models: a proper orthogonal decomposition approach*. PhD dissertation, Eindhoven University of Technology, Department of Electrical Engineering, November 2004.
- [2] P. Astrid, S. Weiland, K.E. Willcox, and A.C.P.M. Backx. Missing point estimation in models described by proper orthogonal decomposition. In *Proceedings of the 43rd IEEE Conference on Decision and Control*, Paradise Island, Bahamas, December 2004.
- [3] P. Astrid, S. Weiland, and A. Twerda. Reduced order modeling of an industrial glass feeder model. In *Proceedings of the 13th IFAC Symposium on System Identification*, Rotterdam, August 2003.
- [4] G. Berkooz and E.S. Titi. Galerkin projections and the proper orthogonal decomposition for equivariant equations. *Physics Letters*, 174:94–102, 1993.
- [5] G.L. Brown and A. Roshko. On density effects and large structures in turbulent mixing layers. *Journal of Fluid Mechanics*, 64:775–816.
- [6] T. Bui-Thanh, M. Damodaran, and K.E. Willcox. Aerodynamic data reconstruction and inverse design using proper orthogonal decomposition. *AIAA Journal*, 42(8):1505–1516, 2004.
- [7] R. Everson and L. Sirovich. The Karhunen-Loève procedure for gappy data. *Journal Opt. Soc. Am.*, 12:1657–1664, 1995.
- [8] P. Holmes, Lumley, and G. Berkooz. *Turbulence, Coherence Structure, Dynamical Systems and Symmetry*. Cambridge University Press, Cambridge, 1996.
- [9] M. Kirby. *Geometric Data Analysis, An Empirical Approach to Dimensionality Reduction and the Study of Patterns*. John Wiley and Sons, Inc, New York, 2001.
- [10] S. Lall, J.E. Marsden, and S. Glavaski. A subspace approach to balanced truncation for model reduction of nonlinear control systems. *International Journal on Robust and Nonlinear Control*, 12(5):519–535.
- [11] H.K. Versteeg and W.K. Malalasekera. *An Introduction to Computational Fluid Dynamics, The Finite Volume Method*. Pearson Prentice Hall, Essex, 1995.
- [12] K.E. Willcox. Unsteady flow sensing and estimation via the gappy proper orthogonal decomposition. In *34th AIAA Fluid Dynamics Conference and Exhibit*, Portland, 2004.